J IRAN CHEM SOC (2017) 14:2263–2273
DOI 10.1007/s13738-017-1163-4

ORIGINAL PAPER

Synthesis, characterization, and antimicrobial and catalytic activity of a new Schiff base and its metal(II) complexes

Halime Güzin Aslan[1] · Senem Akkoç[1] · Zülbiye Kökbudak[1] · Lütfiye Aydın[1]

Received: 28 February 2017 / Accepted: 23 June 2017 / Published online: 15 July 2017

Abstract We presented the synthesis of a new Schiff base and its complexes properties with some transition metal ions in this study. (1-amino-2-thioxo-4-p-tolyl-1,2-dihydropyrimidin-5-yl)(p-tolyl)methanone was synthesized as the starting material, and (1-((2-hydroxynaphthalen-1-yl) methyleneamino)-2-thioxo-4-p-tolyl-1,2-dihydropyrimidin-5-yl)(p-tolyl)methanone (Hnafmmp) (1) and its Ni(II) (2), Pd(II) (3), Pt(II) (4), Cu(II) (5), Co(II) (6) complexes were prepared using above-mentioned starting material. The structures of these new compounds (ligand and its complexes) were characterized with UV–Vis, FTIR, LC–MS, ^{1}H NMR, ^{13}C NMR, magnetic susceptibility, conductivity measurement, X-ray powder diffraction method, and thermal analyses techniques. The ^{1}H NMR chemical shifts of all complexes were calculated by using the gauge-invariant atomic orbital HF (3.21G) method in DMSO phases. All measured results were compared with the experimental data. The ligand and its complexes were also evaluated as antimicrobial agents against representative strains bacteria. Furthermore, we studied the catalytic activity of these compounds in Suzuki–Miyaura cross-coupling reaction in aqueous media.

Keywords Antimicrobial activity · Schiff bases · SAR studies · Suzuki–Miyaura reaction

✉ Halime Güzin Aslan
guzina@erciyes.edu.tr

[1] Faculty of Science, Department of Chemistry, Erciyes University, 33005 Melikgazi, Kayseri, Turkey

Introduction

Research on metal organic complexes represents one of the most active areas of material science and chemical research. Major advances have been made in these materials due to their interesting properties. Schiff bases are some of the most widely used organic compounds in this area. They are used as catalysts, pigments, dyes, polymer stabilizers, and intermediates in organic synthesis [1]. In particular, pyrimidine derivatives have demonstrated a broad range of biological activities, including antimalarial, antifungal, antiproliferative, antibacterial, anti-inflammatory, antiviral, and antipyretic properties and sedative-hypnotic activity [1, 2]. In addition, these derivatives have attracted significant attention because of the application in drug development. Schiff base ligands with sulfur and nitrogen donor atoms in their structures act as good chelating agents for the transition and non-transition of metal ions [3–6]. There is a continuing interest in the metal complexes of Schiff bases. Because of the presence of both hard nitrogen or oxygen and soft sulfur donor atoms in the backbones of these ligands, they readily coordinate with a wide range of transition metal ions yielding stable and intensely colored metal complexes, some of which have been shown to exhibit interesting physical and chemical properties [7] and potentially useful biological activities [8–10].

In this work, we synthesized a new aromatic ligand (1). Subsequently, a series of new Schiff base complexes (1–5) were prepared and characterized by spectroscopic and analytic techniques (Figs. 1, 2). We studied their antibacterial activities against bacteria using the microdilution method. SAR and theoretical studies were performed. The catalytic activities of these compounds were tested in Suzuki–Miyaura cross-coupling reaction. The coupling products were obtained in good yields.

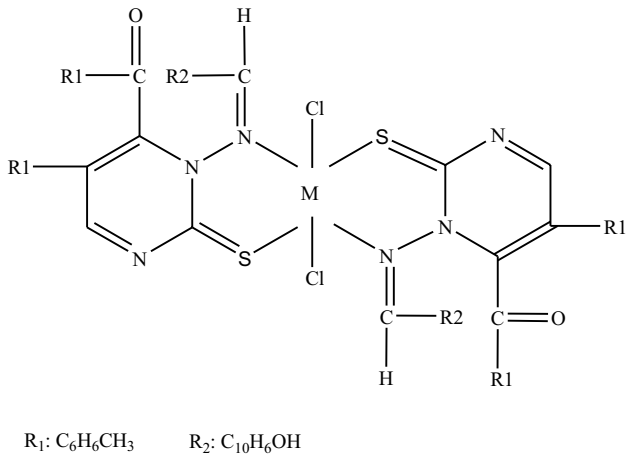

R_1: $C_6H_6CH_3$ R_2: $C_{10}H_6OH$

Fig. 1 Trans (bis(1-((2-hydroxynaphthalen-1-yl)methyleneamino)-2-thioxo-4-p-tolyl-1,2-dihydropyrimidin-5-yl)(p-tolyl)methanone dichloro) M(II) (M: Ni(II)[2], Cu(II)[5], Co(II)[6])

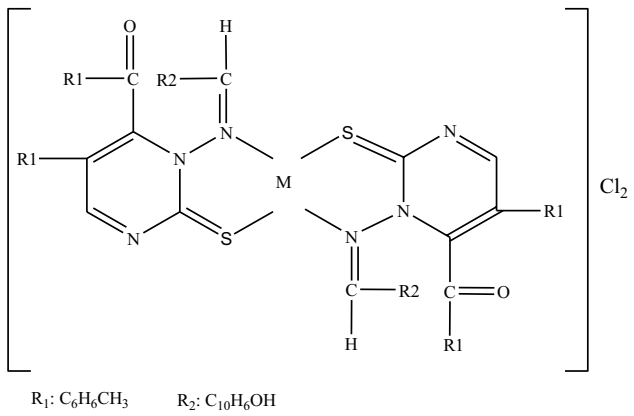

R_1: $C_6H_6CH_3$ R_2: $C_{10}H_6OH$

Fig. 2 Trans (bis(1-((2-hydroxynaphthalen-1-yl)methyleneamino)-2-thioxo-4-p-tolyl-1,2-dihydropyrimidin-5-yl)(p-tolyl)methanone) M(II) Cl_2 (M: Pd(II)[3], Pt(II)[4])

(1-amino-2-thioxo-4-p-tolyl-1,2-dihydropyrimidin-5-yl) (p-tolyl)methanone obtained from (Z)-2-(1-phenylethylidene)hydrazinecarbothioamide with 4-(4-methylbenzoyl)-5-(4-methylphenyl) furan-2,3-dione has been reported before [11]. Schematic representation of the synthesis route of the compound is shown in Scheme 1.

Experimental

Physical measurements

The following instrumental devices were used in this work: Mattson 1000 FTIR spectrometer, AGILENT 1100 (LC–MS), Bruker 400 MHz spectrometer, Bruker AXS D8 diffractometer, Unicam-UV 2-100 spectrometer, PerkinElmer Diamond TG/DTA thermal analyzer, Opti MELT 3 hot-stage apparatus, and Siemens WPA C 35 conductometer.

General procedure for the synthesis

Chemistry of 1

The synthesis of (1-((2-hydroxynaphthalen-1-yl) methyleneamino)-2-thioxo-4-p-tolyl-1,2-dihydropyrimidin-5-yl)(p-tolyl)methanone (1) was carried out according to general pathway illustrated in our previous study [12]. Its details are below: This compound was prepared using (1-amino-2-thioxo-4-p-tolyl-1,2-dihydropyrimidin-5-yl) (p-tolyl)methanone and 2-hydroxy-1-naphthaldehyde. It was obtained as a light-yellow solid, yield 58%; m.p. 203 °C (disintegration); UV (EtOH) λ_{max} (log ε) 520 (3.84) nm; FTIR γ_{max} 3616, 3080, 1639, 764 cm^{-1}; ^1H NMR (DMSO d_6, 400 MHz,): δ: 10.76 (1 H, s), 9.08 (1 H, d, *J*: 8 Hz), 8.90 (1 H), 7.90–6.96 (14 H, m). ^{13}C NMR (DMSO-d_6, 400 MHz,): δ: 191.58, 165.72, 163.87, 160.87, 145.89, 145.14, 141.71, 136.82, 134.20, 133.70, 132.51, 130.61, 130.40, 129.84, 129.59, 129.42, 129.35, 129.31, 128.39, 128.30, 21.67, 21.41. LC/MZ (70 eV, APC1): 490.90 $[M^+ + H^+]$.

Chemistry of 2, 3, 4, 5, 6 complexes

All complexes were prepared by the following standard method [12]. The following results were found:

Bis [(1-((2-hydroxynaphthalen-1-yl)methyleneamino)-2-thioxo-4-p-tolyl-1,2-dihydropyrimidin-5-yl)(p-tolyl) methanone] dichloro nickel(II) (2) was prepared using (1-amino-2-thioxo-4-p-tolyl-1,2-dihydropyrimidin-5-yl) (p-tolyl)methanone, 2-hydroxy-1-naphthaldehyde, and nickel(II)chloride. It was obtained as a light-brown solid, yield 58%; m.p. 220 °C (disintegration); UV (EtOH) λ_{max} (log ε) 514.5 (5.63) nm; FTIR γ_{max} 1618, 1280, 751 cm^{-1}; ^1H NMR (DMSO-d_6, 400 MHz,): δ: 10.72 (1 H, s), 10.25 (1 H, s), 9.61 (2 H, d, *J*: 8 Hz), 8.30 (2 H), 7.99–5.38 (28 H, m), 2.66 (2 H, m, *J*: 12 Hz), 2.49 (2 H, m, *J*: 12 Hz), 2.35 (2 H, m, *J*: 12 Hz), 2.27 (2 H, m, *J*: 12 Hz), 2.16 (2 H, m, *J*: 12 Hz), 2.07 (2 H, m, *J*: 12 Hz). ^{13}C NMR (DMSO-d_6, 400 MHz,): δ: 193.22, 164.73, 145.17, 145.08, 141.70, 138.86, 134.02 (2C), 130.88 (4C), 130.62 (4C), 130.42, 130.23, 129.86, 129.78, 129.60, 129.40, 124.69, 124.56, 122.71, 119.19, 21.79, 21.66, 21.42, 21.30. LC/MZ(70 eV, APC1): 1039.70 $[M^+ + 2H^+]$.

Bis [(1-((2-hydroxynaphthalen-1-yl)methyleneamino)-2-thioxo-4-p-tolyl-1,2-dihydropyrimidin-5-yl)(p-tolyl) methanone] palladium(II) chloride (3) was prepared using [(1-amino-2-thioxo-4-p-tolyl-1,2-dihydropyrimidin-5-yl) (p-tolyl)methanone], 2-hydroxy-1- naphthaldehyde, and

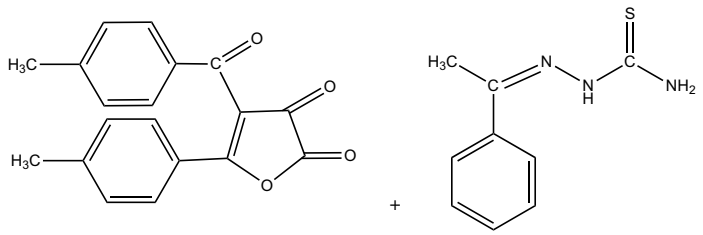

4-(4-methylbenzoyl)-5-(4-methylphenyl)furan-2,3-dione + (*Z*)-2-(1-phenylethylidene)hydrazinecarbothioamide

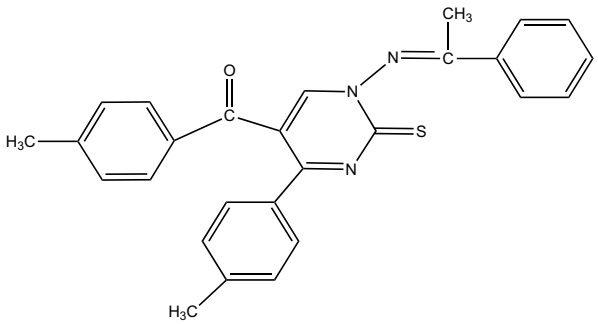

(*Z*)-(1-(1-phenylethylideneamino)-2-thioxo-4-*p*-tolyl-1,2-dihydropyrimidin-5-yl)(*p*-tolyl)methanone

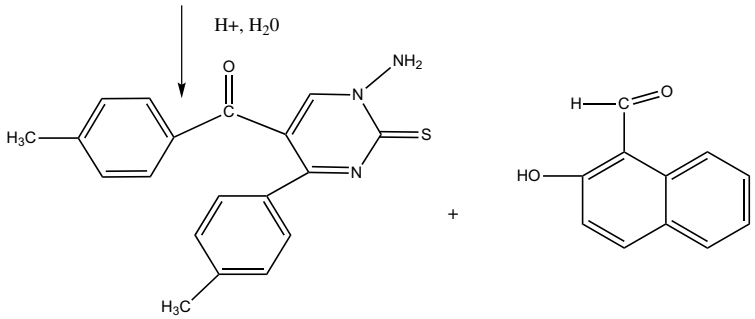

(1-amino-2-thioxo-4-*p*-tolyl-1,2-dihydropyrimidin-5-yl)(*p*-tolyl)methanone + 2-hydroxy-1-naphthaldehyde

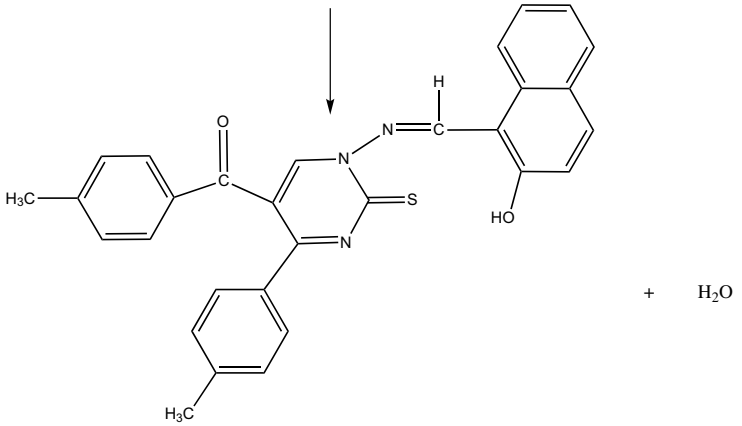

(1-((2-hydroxynaphthalen-1-yl)methyleneamino)-2-thioxo-4-*p*-tolyl-1,2-dihydropyrimidin-5-yl)(*p*-tolyl)methanone

Scheme 1 (1-((2-hydroxynaphthalen-1-yl)methyleneamino)-2-thioxo-4-p-tolyl-1,2-dihydropyrimidin-5-yl)(p-tolyl)methanone 's reaction mechanism

palladium(II) chloride. It was obtained as a reddish-brown solid, yield 52%; mp 206 °C (disintegration); UV (EtOH) λ_{max} (log ε) 514.5 (5.63) nm; FTIR γ_{max} 751, 1279, 1600 cm^{-1}; ^1H NMR (DMSO-d_6, 400 MHz,): δ: 10.76 (1 H, s), 10.75 (1 H, s), 9.08 (1 H, s), 9.07 (1 H, s), 8.91 (1 H, s), 8.90 (1 H, s), 7.89–7.25 (28 H, m), 2.53 (2 H, d, *J*:

8 Hz), 2.49 (2 H, d, *J*: 8 Hz), 2.41 (2 H, d, *J*: 12 Hz), 2.35 (2 H, d, *J*: 12 Hz), 2.32 (2 H, d, *J*: 12 Hz), 2.31 (2 H, d, *J*: 12 Hz), 2.27 (2 H, d, *J*: 12 Hz), 2.26 (2 H, d, *J*: 12 Hz), 2.24 (2 H, d, *J*: 12 Hz), 2.18 (2 H, d, *J:* 12 Hz), 2.16 (2 H, d, *J*: 12 Hz). ^{13}C NMR (DMSO-d_6, 400 MHz,): δ: 193.12, 191.59, 176.38, 164.53, 145.95, 144.16, 143.49, 141.69, 138.77, 134.19, 133.70, 132.47, 132.08, 130.96, 130.62, 130.22, 130.06, 129.95, 129.75, 129.59, 129.42, 129.26, 124.65, 122.81, 120.77, 119.24, 39.32, 21.75, 21.68, 21.41. LC/MZ (70 eV, APC1): 1086.59 [$M^+ + H^+$].

Bis [(1-((2-hydroxynaphthalen-1-yl)methyleneamino)-2-thioxo-4-p-tolyl-1,2-dihydropyrimidin-5-yl)(p-tolyl) methanone] platinum(II) chloride (4) was prepared using [(1-amino-2-thioxo-4-p-tolyl-1,2-dihydropyrimidin-5-yl)(p-tolyl)methanone], 2-hydroxy-1- naphthaldehyde, and platinum(II) chloride. It was obtained as a reddish-brown solid, yield 44%; m.p. 291 °C (disintegration); UV (EtOH) λ_{max} (log ε) 344.6 (5.33) nm; FTIR γ_{max} 750, 1280, 1602 cm^{-1}; ^{1}H NMR (DMSO-d_6, 400 MHz,): δ: 10.00 (1 H, s), 10.01 (1 H, s), 8.90 (1 H, s), 8.80 (1 H, s), 8.70 (1 H, s), 8.60 (1 H, s), 8.30–6.80 (28 H, m) 2.49 (2 H, d, *J*: 8 Hz), 2.41 (2 H, d, *J*: 12 Hz), 2.37 (H, s), 2.33 (H, s), 2.31 (H, s), 2.29 (H, s), 2.26 (H, s), 2.24 (H, s), 2.18 (H, s), 2.16 (H, s). ^{13}C NMR (DMSO-d_6, 400 MHz,): δ: 193.21, 192.49, 175.28, 164.55, 146.95, 144.22, 143.54, 141.80, 139.22, 134.23, 133.81, 132.39, 132.05, 131.06, 130.80, 130.32, 130.04, 130.05, 129.88, 129.49, 129.40, 129.15, 124.45, 122.92, 121.07, 119.22, 39.32, 21.80, 21.88, 21.54.LC/MZ(70 eV, APC1): 1175.25 [$M^+ + H^+$].

Bis [(1-((2-hydroxynaphthalen-1-yl)methyleneamino)-2-thioxo-4-p-tolyl-1,2-dihydropyrimidin-5-yl)(p-tolyl)methanone] dichloro cupper(II) (5) was prepared using [(1-amino-2-thioxo-4-p-tolyl-1,2-dihydropyrimidin-5-yl)(p-tolyl) methanone], 2-hydroxy-1-naphthaldehyde, and cupper(II) chloride. It was obtained as a light-brown solid, yield 48%; m.p. 176 °C (disintegration); UV (EtOH) λ_{max} (log ε) 475.8 (5.59) nm; FTIR γ_{max} 1602, 1280, 759 cm^{-1}. ^{1}H NMR ($DMSOd_6$, 400 MHz,): δ: 11.86 (1 H, s), 11.81 (1 H, s), 9.92 (1 H, s), 9.86 (1 H, s), 9.76 (1 H, s), 9.59 (1 H, s), 9.56–6.60 (28 H, m), 2.85 (2 H, d, *J*: 8 Hz), 2.80–2.29 (10 H, m). ^{13}C NMR (DMSO-d_6, 400 MHz,) δ: 191.58, 160.91, 145.93, 145.15, 141.73, 134.19, 130.65, 130.24, 129.96, 129.63, 129.44, 128.99, 128.28, 124.60, 119.12, 25.62, 21.82, 21.48, 20.80.LC/MZ(70 eV, APC1): 1044.70 [$M^+ + 2H^+$].

Bis [(1-((2-hydroxynaphthalen-1-yl)methyleneamino)-2-thioxo-4-p-tolyl-1,2-dihydropyrimidin-5-yl)(p-tolyl) methanone] dichloro cobalt(II) (6) was prepared using [(1-amino-2-thioxo-4-p-tolyl-1,2-dihydropyrimidin-5-yl) (p-tolyl)methanone], 2-hydroxy-1-naphthaldehyde, and cobalt(II) chloride. It was obtained as a dark-brown solid, yield 51%; m.p. 199 °C (disintegration); UV (EtOH) λ_{max} (log ε) 320.2 (5.42) nm; FTIR γ_{max} 1602, 1280, 751 cm^{-1}. ^{1}H NMR (DMSO-d_6, 400 MHz,): δ: 11.99 (1 H, s), 11.80 (1 H, s), 9.84 (1 H, s), 9.71 (1 H, s), 9.16 (1 H, s), 8.88(1 H, s), 8.76 (2 H, t, *J*: 4 Hz), 8.73 (2 H, t, *J*: 12 Hz), 8.10 (2 H, t, *J*: 8 Hz), 8.08 (2 H, t, *J*: 8 Hz), 8.06 (4 H, t, *J*: 8 Hz), 8.02 (4 H, t, *J*: 16 Hz), 8.00 (4 H, t, *J*: 8 Hz), 7.91 (4 H, t, *J*: 36 Hz), 7.89 (2H, t, *J*: 12 Hz), 7.86 (2 H, t, *J*: 12 Hz), 7.84 (2 H, t, *J*: 8 Hz), 7.82 (2 H, t, *J*: 8 Hz) 7.79 (1 H, d, *J*: 16 Hz), 7.77 (4 H, d, *J*: 8 Hz), 7.73 (4 H, d, *J*: 24 Hz), 7.65 (4 H, d, *J*: 8 Hz), 7.63 (1 H, d, *J*: 8 Hz), 7.61 (2 H, d, *J*: 8 Hz), 7.59 (1 H, d, *J*: 12 Hz), 7.57 (1 H, d, *J*: 8 Hz), 7.55 (1 H, d, *J*: 8 Hz), 7.53 (1 H, d, *J*: 12 Hz), 7.44 (1 H, d, *J*: 4 Hz), 7.42 (1 H, d, *J:* 8 Hz), 7.40 (2 H, t, *J:* 4 Hz), 7.38 (2 H, t, *J*: 81 Hz), 7.36 (2 H, t, *J*: 8 Hz), 7.34 (2 H, t, *J*: 8 Hz), 2.53 (3 H, m), 2.49 (3 H, m), 2.36 (3 H, m), 2.32 (3 H, m). ^{13}C NMR (DMSO-d_6, 400 MHz,) δ: 191.80, 165.37, 147.94, 144.59, 141.23, 134.75, 132.34, 130.47, 130.24, 129.76, 129.59, 129.38, 129.15, 128.94, 128.35, 124.50, 123.72, 119.00, 116.04, 108.66, 107.73, 107.53, 39.93, 21.66, 21.39. LC/MZ(70 eV, APC1): 1038.10 [M^+].

Biological activity evaluation

The procedures of antimicrobial activity study were performed according to the literature [12].

Minimal inhibitory concentration

Minimal inhibitory concentrations (MIC) [13–17] were determined by the microdilution broth method following the procedures recommended by the National Committee for Clinical Laboratory Standards (NCCLS, 2000). Trimethoprim and tetracycline were used as standard drugs.

General procedure for the Suzuki–Miyaura cross-coupling reaction

Compounds (0.03 mmol), aryl chloride (1 mmol), phenylboronic acid (1.5 mmol), base (2.0 mmol), and H_2O/DMF (2/2 mL) were added to a small Schlenk tube, and the reaction mixture was heated up to various temperature for different time. At the end of the reaction, the mixture was cooled, extracted with ethyl acetate/hexane (1:5), and purified by flash chromatography on silica gel. The purity of the compounds was checked by GC–MS. Conversions were based on aryl chlorides.

Results and discussion

This report presented the synthesis, characterization, biologic, catalytic, and spectral studies of the ligand (1) and its five new nickel, palladium, platinum, copper, and cobalt complexes. According to FTIR, ^{1}H NMR, and X-ray powder diffraction's data, an octahedral geometry is observed

around the nickel, copper, cobalt complexes and a square planar geometry around the palladium and platinum complexes, in which the ligand acts as a neutral bidentate one, coordinating through its nitrogen and sulfur atoms. In reality, ligand has carbonyl and hydroxyl groups. These groups are more effective than C=S group. Conversely, these attachment points are expected for complexation reactions. But according to ^{1}H NMR results, the phenolic –OH signals of all compounds are determined between 10.26 and 10.79 ppm, and C=O signals are determined between 163–171 ppm and ^{1}H NMR spectra of the free ligand task to (C=O) is not shifted. In IR spectra, ʊ(C=N) and ʊ(C=S) groups signals are shifted to –35, −63 cm^{-1} and −21, −39 cm^{-1}, respectively. However, there is no shifting by –OH and C=O signals. This situation was investigated using Gaussian software program. The total energies were calculated with the HF (3.21G) method for each case. We have calculated less energy values when connected via sulfur atoms.

The results showed 1:2 (metal/ligand) stoichiometric for all the complexes and two additional values for the chloride ligands which is coordinated to the metal atoms (only Ni, Cu, Co). Ni(II), Cu(II), and Co(II) complexes have an octahedral geometry and Pd(II), Pt(II) complexes have a square planar geometry. However, in our previous studies [18, 19], an octahedral geometry was observed around the Cu(II) and Co(II) complexes and a square planar geometry for Ni(II), Pd(II), and Pt(II) complexes. All complexes found to be stable at room temperature in their solid states and generally soluble in CH_2Cl_2, DMSO, and DMF. According to these observed results, the nickel, cobalt, and copper complexes have a non-electrolytic nature. The platinum and palladium complexes have an electrolytic nature.

FTIR spectra

The –NH stretching vibrations were occurred at 3300–3500 cm^{-1}. In here, the –NH stretching vibration was observed at 3450 cm^{-1} for (1). The aromatic structure showed the presence of –CH stretching vibrations in the range 3000–3100 cm^{-1}, which is the characteristic region for –CH stretching. The –CH asymmetric stretching vibrations were observed at 3072 cm^{-1} for compound 1. The IR spectrum of compound (1) showed characteristic stretching bands corresponding to the carbonyl groups. These bands were observed at 1647 cm^{-1}. The IR spectra of the Schiff base ligand showed a broad band at 3616 cm^{-1} [20]. Due to intramolecular hydrogen bonding between the H of OH and the azomethine nitrogen, this band was observed in low frequency (3080 cm^{-1}). The IR spectra of the free ligand observed strong bands at 1639 and 764 cm^{-1} assigned to ʊ(C=N) and ʊ(C=S). These bands shifted to −39, −21 cm^{-1}, and −14, −5 cm^{-1}, respectively. These are indicating coordination via the azomethine nitrogen and thiocarbonyl of the Schiff base.

NMR spectra

DMSO used as a solvent to measure the ^{1}H NMR spectra of 1 and its complexes. The sharp singlet peak was observed at 10.76 ppm, which is assigned to the phenolic proton of the ligand. The phenyl was observed as multiplet between 7.83 and 6.95 ppm. The azomethine proton and the pyrimidine ring (C–H) proton assigned as singlet at 9.08 and 8.90 ppm, respectively. The chemical shift values of the different types of protons in the examined compounds (1 and 2) are reported in Figs. 3 and 4.

In ^{13}C NMR spectrum, the aromatic C peaks were observed between 117.26 and 145.84 ppm. The azomethine C and the pyrimidine ring C in the spectrum of 1 assigned at 190.65–192.25 and 155.07–171.84 ppm, respectively. The methyl carbons were observed in between 19.04 and 21.91 ppm.

The theoretical studies of ^{1}H NMR were conducted with the HF (3.21G) method by Gaussian software program, and it was compared with the experimental data (Fig. 5). There are good correlations between theoretical and experimental results. However, hydrogen belonging to pyrimidine rings, hydrogen belonging to salycyl aldehyde's, and hydrogen belonging to hydroxyl group of these complexes chemical shifts differ from theoretical chemical shifts. These results can be explained by the presence of an intramolecular hydrogen bond. The electronic charge density around of these atoms changes rapidly due to the influence of the hydrogen bridge bond or

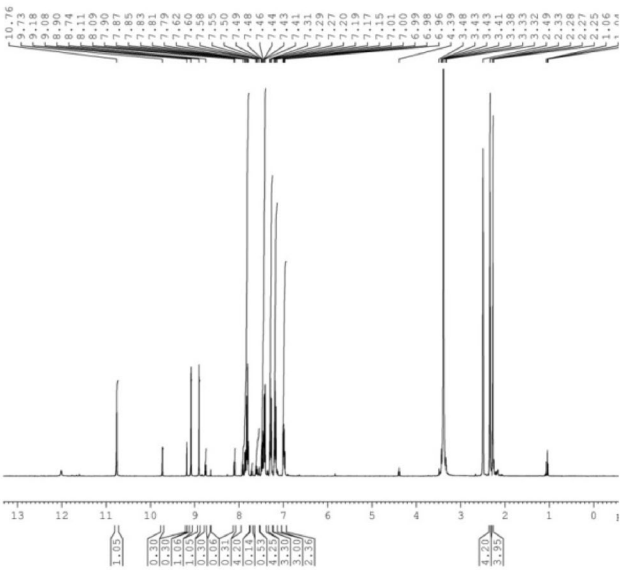

Fig. 3 ^{1}H NMR diagram of 1

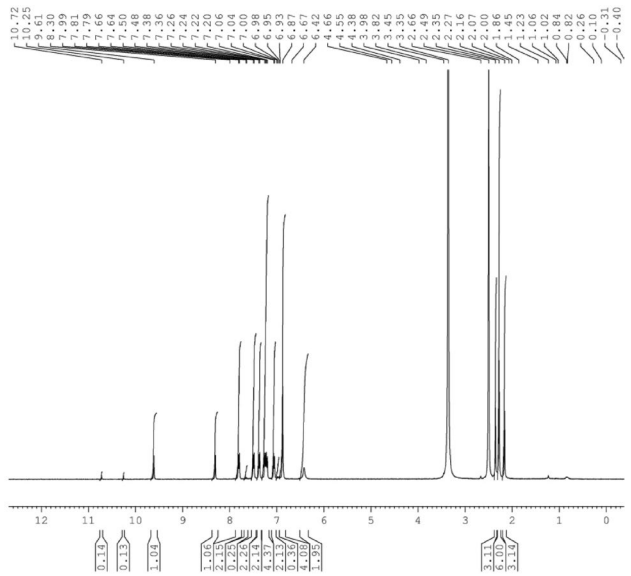

Fig. 4 ^{1}H NMR diagram of 2

solvent effect. The chemical shift values of these hydrogens have been subtracted from the graph because of the above-mentioned reasons.

UV spectra

Experimental UV parameters and suggested geometries for complexes are presented in the Table 1 [21].

LC–MS spectra

LC/MS showed that Cu (5) and Co (6) complex give the molecular ion [M^+] at 1038.7 and 1042.3 m/z, respectively. The Ni complex (2) gave the molecular ion [M^+] + 2H^+ at 1037.9 m/z. The Pd and Pt complexes (3, 4) gave the molecular ions, [M^+] + H^+ at the desired positions at 1089.59 and 1174.25 m/z. Separately, all complexes and ligand gave the fragmentation of the C_6H_5 group, which was observed at 79.2 m/z.

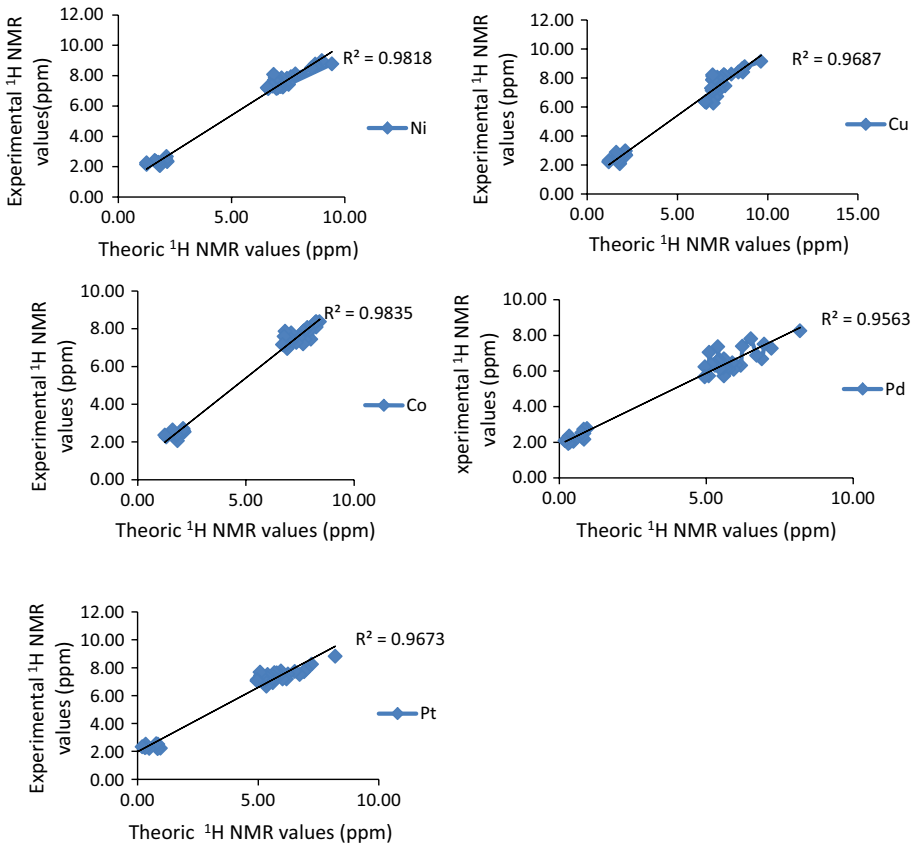

Fig. 5 Correlation graphs between the experimental and theoretical chemical shifts results

Table 1 UV determination results of all synthesized complexes

Complexes	Ni(2)	Pd(3)	Pt(4)	Cu(5)	Co(6)
Magnetic Moment value (B.M.)	3.67	0.15	0.30	2.33	4.82
Observed band (nm)	514.5	514.5	344.6	475.8	320.2
Transitions	$^3T_{1g} \rightarrow {}^3T_{1g}(P)$	$^1A_{1g} \rightarrow {}^1E_g$	$^1A_{1g} \rightarrow 3B_{1g}$	$^2B_{1g} \rightarrow {}^2E_g$	$^4T_{1g}(P) \rightarrow {}^4A_{2g}$
Recommended geometry	Octahedral	Square planar	Square planar	Octahedral	Octahedral

X-ray powder diffraction

The powder patterns of the ligand (Hnafmmp) were indexed in orthorhombic crystal systems with unit cell parameters of a: 12.91, b: 10.55, c: 9.878 Å. Compound **2** was indexed in an orthorhombic crystal system with unit cell dimensions of a: 13.03, b: 12.59, c: 8.75 Å. Compound **3** was indexed in an orthorhombic crystal system with unit cell dimensions of a: 6.39, b: 3.17, c: 2.00 Å. Compound **4** was indexed in a cubic crystal system with unit cell dimensions of a: 3.14 Å. Compound **5** was indexed in an orthorhombic crystal system with unit cell dimensions of a: 16.93, b: 10.27, c: 8.88 Å. Compound **6** was indexed in orthorhombic crystal system with unit cell dimensions of a: 15.78, b: 14.38, c: 6.66 Å.

Thermal studies

TG/DTA analyses for the compounds were taken in nitrogen at the temperature from 50 to 1200 °C. Compounds 1 and 3 were discussed as detail. The thermal decomposition of 1 ($C_{30}H_{23}SO_2N_3$) takes place in three stages. Firstly, $–CHC_{10}H_6OH$ group degrades at 200 °C, shown as one maximum in the DTG curve at 195.26 °C with 30.00% mass loss (calc. = 31.84%). Secondly, one mole of the $–C_6H_5CH_3$ and one mole of the $–COC_6H_5CH_3$ groups have been degraded. It shows one peak at 207.57 °C in DTG curve for this stage. Third stage is related to the decomposition, and this stage finishes at 1200 °C. The $[C_{60}H_{46}N_6O_4S_2Cl_2Pt]$ complex is thermally decomposed in four stages. Firstly, from 0 to 200 °C, two moles of chloride molecules degrade, shown as one maximum in the DTG curve at 200.00 °C with a 5.77% mass loss (calc. = 5.62%). Second stage's mass loss of 25.34% is due to the degradation of two moles of $–CHC_{10}H_6OH$ molecules, which is in agreement with the calculated value (calc. = 25.06%). The DTG curve shows one peak at 290.00 °C. The third stage's mass loss of 70.94% is due to the degradation of two moles of $–COC_6H_5CH_3$, two moles of $–C_6H_5CH_3$, two moles of –N, and two moles of –S molecules, which is in agreement with the calculated value (calc. = 71.81%). The DTG curve shows one peak at 310.00 °C. The last stage is related to the decomposition of the remaining part of the complex molecule. The total residue (calc. = 15.67%) is Pt (ECPDS number: 04-0802). The residue indexed in a cubic crystal system with unit cell dimensions of a: 3.9231 Å. The thermal behaviors of the compounds are presented in Table 2.

The DTA/TG curves of the ligand (*L*) and its complexes are shown in Fig. 6.

Conductometric measurements

Measurements were taken at 25 °C in 10^{-3} M DMSO solutions using a conductivity meter. The complexes 2, 5, and 6 dissolve in DMSO to give a total one ion. These complexes did not have an electrolytic nature. The molar conductivity of complexes 2, 5, and 6 are 48, 32, and 70 S/M, respectively. The platinum and palladium complexes molar conductivity were found as 256 and 254 S/M, respectively.

Antimicrobial activity

Ligand and its complexes were evaluated by the microdilution method procedure for their in vitro antibacterial activity. All the compounds displayed activity against *M. luteus*, *P. mirabilis*, *P. aeruginosa*, and *C. renale*. On the other hand, none of the compounds displayed activity against *E. aerogenes* and *S. epidermidis* bacteria. *E. aerogenes* and *S. epidermitis* are pathogenic bacterium. They cause opportunistic infections; these include most types of infections. *E. aerogenes* quickly become resistant to standard antibiotics during treatment. *S. epidermitis* lives on the human skin and mucosa. It has ability to form biofilms on plastic devices and the most common infections on catheters and implant. The Cu, Ni, Pt complexes and Hnafmmp generally seemed to be more active against gram-positive bacteria. But, the Co and Pd complexes displayed poor activity against all gram-positive and gram-negative bacteria. This situation is contrary to with previous studies, where the ligand and its Pd and Pt complexes were found to be more

Table 2 Thermal behaviors of 1 and its complexes

Substance	Peak temp. in DTG/°C	Temp. ranges in TG/°C	Mass TG theoretical	Loss%	Evolved moiety	Residue (ECPDS number)
Hnafmmp	195.26	0–200	30.00	31.84	–CH–$C_{10}H_6OH$	–
	207.57	200–300	75.00	74.70	–CO–$C_{10}H_6CH_3$ –$C_{10}H_6CH_3$	
	1200	600–1200	99.00	99.00	Remaining part of ligand	
[Ni(1)$_2$Cl$_2$]	201.32	0–200	7.00	6.95	–2–Cl	NiO
	260.33	250–300	67.00	64.20	–2–$CHC_{10}H_6$–OH	(44-1159)
	1254.49	350–1300	71.00	72.35	–2 $COC_6H_5CH_3$, −2 $C_6H_5CH_3$	Hexagonal
[Co(1)$_2$Cl$_2$]	203.78	0–200	5.57	6.32	–2–Cl	CoO·Co_2O
	293.78	300–400	28.54	28.18	–2–CH–$C_{10}H_6OH$	(02-1079)
	853.78	400–850	74.55	74.43	–2–CH–$C_{10}H_6OH$ –2–$COC_{10}H_6CH_3$, –2–$C_{10}H_6CH_3$, –2–N, –2–S	Face centered cubic
	953.78	850–1000	21.88	21.71	Residue	
[Cu(1)$_2$Cl$_2$]	184.75	0–200	6.54	6.23	–2–Cl	CuO (tenorite)
	294.75	300–400	29.08	28.04	–2–CH–$C_{10}H_6OH$	(01-1117)
	704.75	400–800	74.03	73.08	–2–CH–$C_{10}H_6OH$ –2–$COC_{10}H_6CH_3$, –2–$C_{10}H_6CH_3$, –2–N, –2–S	Monoclinic
	1174.75	850–1300	7.329	7.147	CuO residue	
[Pd(1)$_2$]Cl$_2$	184.91	0–200	5.92	6.05	–2–Cl	PdS
	364.91	300–400	33.30	33.03	–2–CH–$C_{10}H_6OH$	(74-1060),
	1124.91	400–1200	77.42	77.32	–2–CH–$C_{10}H_6OH$ –2–$COC_{10}H_6CH_3$, –2–$C_{10}H_6CH_3$, –2–N, –2–S	Tetragonal
	1254.91	1200–1300	15.00	13.00	Residue	
[Pt(1)$_2$]Cl$_2$	200.00	0–200	5.77	5.62	–2–Cl	Pt
	290.00	200–400	25.34	25.06	–2–CH–$C_{10}H_6OH$	(04-0802)
	310.00	200–400	70.94	71.81	–2–CH–$C_{10}H_6OH$ –2–$COC_{10}H_6CH_3$, –2–$C_{10}H_6CH_3$, –2–N, –2–S	Cubic
	1174.75	850–1300	15.60	15.67	Residue	

active against gram-negative and gram-positive bacteria [18, 19]. The biological activity results displayed that complex 5(Cu(II)) provided good protection against convulsions while complex 2(Ni(II)) is significantly less active. The differences between the high and the low active complexes consist of the amount of distribution of the negative electrostatic potential around the sulfur and nitrogen atoms. Complex **5** had a high value for the negative electrostatic potential around the sulfur and nitrogen atoms, which is the most potent compound. On the other hand, complex 2 had lower negative electrostatic potential around its sulfur and nitrogen atoms, which is the very least active compound. This is evident in the electrostatic maps of the two complexes in Fig. 7.

The molecular electrostatic potential maps for the two complexes are shown in Fig. 7. The optimized geometries of complexes are shown in Fig. 8. The antimicrobial activity results are given in Table 3.

SAR analysis

The parameters of the synthesized compounds were selected. The chemical structures of the compounds are set up with the GAUSSIAN 3.0 program and optimized with

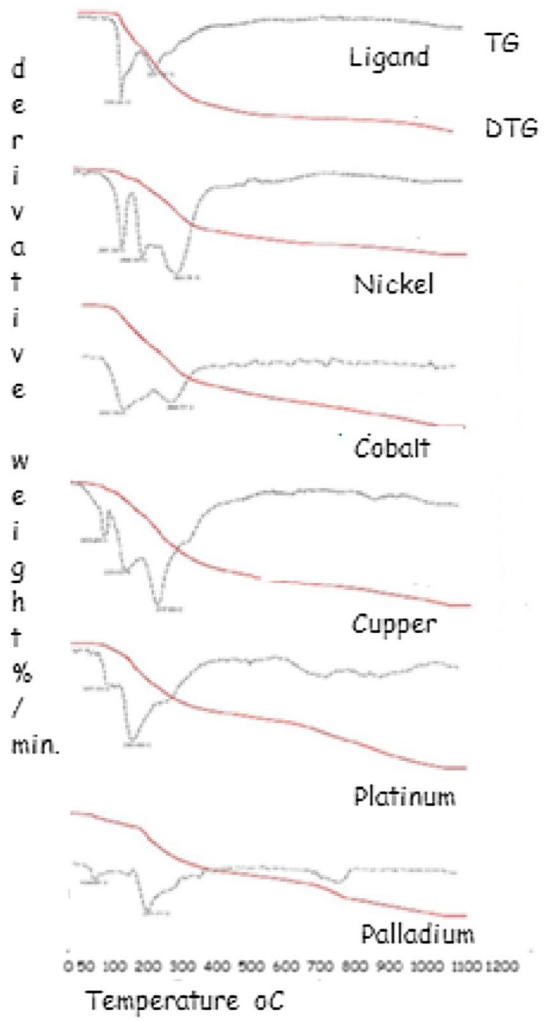

Fig. 6 DTA/TG curves of the ligand and its complexes (x-axis shows temperature, and y-axis shows % weight)

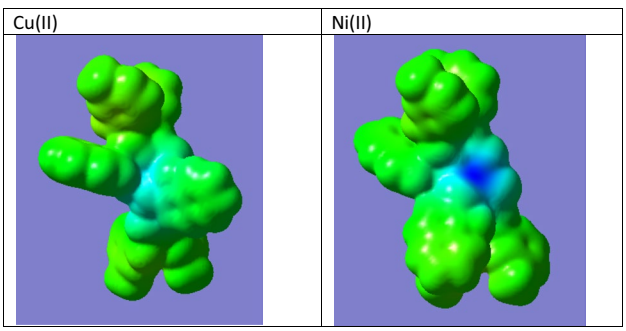

Fig. 7 Electrostatic potential maps for Cu(II) and Ni(II) complexes (*dark blue* is electropositive potential)

the HF (3.21G) method. HOMO and LUMO were calculated and founded values are given in Table 4.

The treatment of the HOMO and LUMO is based on the general principles governing the nature of reactions. The LUMO energy is related to the electron affinity susceptibility of the molecule toward attack by nucleophiles. On the other hand, hard and soft nucleophiles have been directly related to the energy of HOMO–LUMO: hard electrophiles have a high energy. LUMO and soft electrophiles have a low energy. There was a linear relationship between LUMO-*L. monocytogenes* and HOMO-*L. monocytogenes* where R^2 was obtained as 0.992 and 0.993, respectively (Figs. 9, 10).

Catalytic activities in Suzuki–Miyaura reaction

First experiment was performed with phenylboronic acid and 4-chloroacetophenone as model compounds to find optimum conditions. The coupling product **1** was obtained in 70% conversion in **4** catalyst (Table 5, entry 1). After that, to assure this tendency, two catalysts were used in the same reaction, and good conversions were obtained such as 61%. Then, 4-chloroanisole was reacted with phenylboronic acid by using these novel complexes (Table 5, entries 4–8). For this transformation, complexes **5, 6,** and **4** were found to be effective catalysts at 80 °C for 2 h. The coupling of phenylboronic acid with chlorobenzene was observed to proceed under a variety of conditions. Two different bases (K_2CO_3 and NaOH) and solvents (DMF and H_2O) as well as synthesized novel compound (**6**) were employed. When two bases were used, good results were obtained. At low time and temperature, NaOH was used as a base and achieved very good result such as 80% conversion. Therefore, both K_2CO_3 and NaOH were a good choice in DMF/H_2O systems as a base. Water was used as solvent in this coupling reaction. When Table 5 is examined, it is seen that the results of the Suzuki–Miyaura cross-coupling reaction are between 34 and 95. As a result of this study, we concluded that 4 and 5 complexes in the Suzuki–Miyaura coupling reactions showed high activity in comparison with other complexes. As a result, synthesized complexes are found to be effective Suzuki–Miyaura cross-coupling reactions. In our previous study, the catalytic activities in the end Suzuki–Miyaura coupling (DMF-H_2O) reactions of synthesized compounds were examined [22, 23] and obtained similar results in this study.

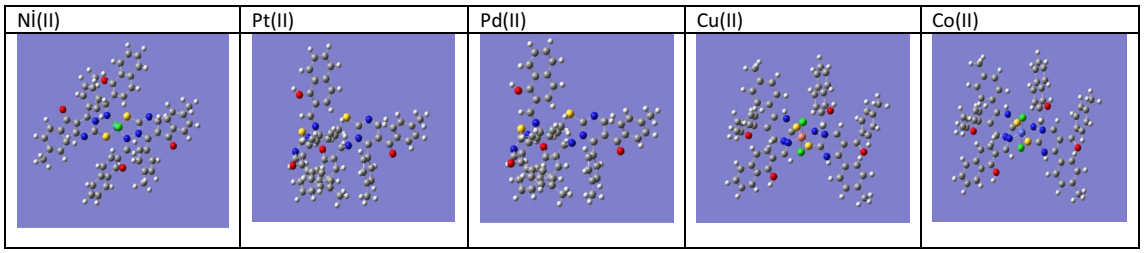

Fig. 8 Optimized geometries of complexes

Table 3 Microdilution assays (μM) of compound and reference antibiotics against tested microorganisms by the microdilution method

	1	2	3	4	5	6	Trimethoprim (μM)	Tetracycline (μM)
−*P. fluorescens*	0.54	2.02	0.48	0.23	0.26	2.67	0.34	0.03
−*P. aeruginosa*	2.14	2.02	0.96	0.89	2.01	1.01	0.34	0.03
−*E. coli*	2.14	2.02	1.93	1.79	2.01	2.02	–	0.02
−*K. pneumonia*	4.29	2.02	1.93	0.89	0.50	2.02	0.34	0.03
−*E. aerogenes*	4.29	2.02	1.93	1.79	2.01	2.02	0.34	0.03
+*S. aureus*	4.29	1.01	1.93	1.79	2.01	2.02	–	0.22
+*B. cereus*	4.29	2.02	1.93	0.89	0.50	2.02	–	–
+*S. epidermidis*	4.29	2.02	1.93	1.79	2.01	2.02	–	0.03
+*E. faecalis*	4.29	2.02	1.93	1.79	1.00	2.02	0.17	0.14
+*B. subtilis*	2.14	2.02	1.93	1.79	2.01	2.02	0.34	0.02
+*M. luteus*	4.29	1.01	1.93	0.89	1.00	0.51	0.69	0.11
+*L. monocytogenes*	4.29	2.02	0.48	0.89	1.00	2.02	0.01	0.01
−*P. mirabilis*	1.07	2.02	0.48	1.79	0.50	1.01	–	–
+*C. renale*	1.07	1.01	0.96	0.89	1.00	1.01	–	–

Table 4 HOMO and LUMO energy values of the synthesized compounds

Compound	HOMO	LUMO
Ligand	−0.00200	0.0041
Ni(II)	−0.00188	0.0037
Pd(II)	−0.00846	0.0005
Pt(II)	−0.00081	0.0016
Cu(II)	−0.00590	0.0017
Co(II)	−0.00130	0.0039

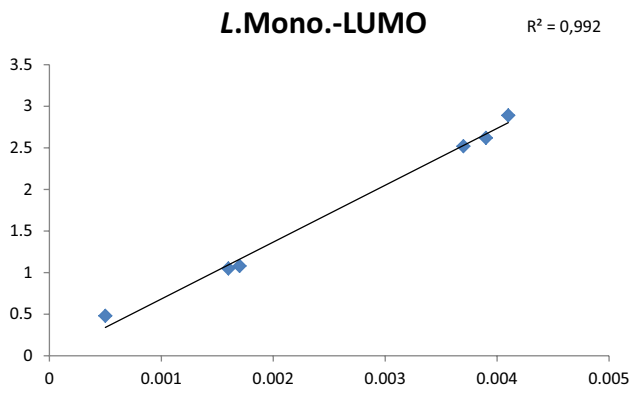

Fig. 9 Relationship with MIC(*L.* Monocytogenes) and LUMO

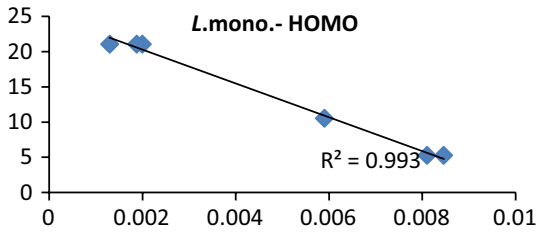

Fig. 10 Relationship with MIC (*L.* Monocytogenes) and HOMO

Conclusion

As conclusion, one ligand and its complexes were synthesized and characterized. From the spectroscopic characterization, it was concluded that compound 1 acts as a bidentate ligand, coordinating through –C=N and –S. The Ni(II), Co(II), and Cu(II) complexes had an octahedral geometry, and Pd(II), Pt(II) complexes had a square planar geometry. Compound 1 (Hnafmmp) was indexed in orthorhombic crystal systems with unit cell parameters of a: 12.91, b: 10.55, c: 9.878 Å. Complexes 2, 3, 4, 5 and 6 were indexed in an orthorhombic, an orthorhombic, a cubic, an orthorhombic, and an orthorhombic crystal systems, respectively. The thermal decomposition of compound 1

Table 5 Suzuki–Miyaura coupling reaction of phenylboronic acid by using aryl chlorides

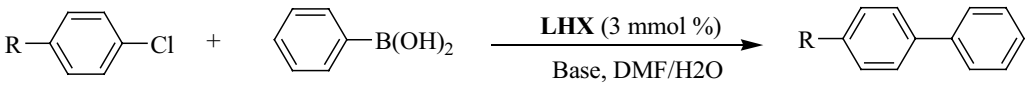

Entry	R	LHX	Product	Time (min)	Temperature (°C)	Base	Yield (%)
1	$COCH_3$	**4**	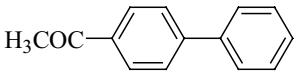	120	80	K_2CO_3	70
2	$COCH_3$	**2**		120	80	K_2CO_3	61
3	OCH_3	**5**	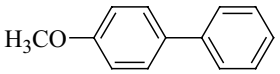	120	80	K_2CO_3	91
4	OCH_3	**3**		120	80	K_2CO_3	34
5	OCH_3	**2**		120	80	K_2CO_3	54
6	OCH_3	**6**		120	80	K_2CO_3	80
7	OCH_3	**4**		120	80	K_2CO_3	95
8	H	**6**	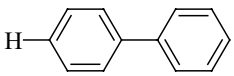	120	80	K_2CO_3	72

Reaction conditions: p-R-C_6H_4Cl (1.0 mmol), phenylboronic acid (1.5 mmol), Base (2.0 mmol), **1** (2.0 mmol%), water (2 mL)-DMF (2 mL). Purity of compounds is checked by NMR. All reactions were monitored by GC spectroscopy, and yields are based on aryl chloride

($C_{30}H_{23}SO_2N_3$) takes place in three stages. The complexes with the molecular formula [$C_{60}H_{46}N_6O_4S_2Cl_2M$] (M, Ni(II), Pd(II), Pt(II), Cu(II), Co(II)) were thermally decomposed in four stages. All compounds demonstrated biological activity against all the tested strains. Tested compounds in Suzuki–Miyaura cross-coupling reactions for catalytic activities gave very good conversions. ^{1}H NMR studies of these complexes were calculated as theoretically.

Acknowledgements The authors are grateful to Erciyes University's Research Foundation for financial support under project number EUBAP-FBA-09-975.

References

1. D.N. Dhar, C.L. Taploo, J. Sci. Ind. Res. **41**, 501 (1982)
2. P. Przybyslki, A. Huczynski, K. Pyta et al., Curr. Org. Chem. **13**, 124 (2009)
3. N.K. Kaushik, A.K. Mishra, Ind. J. Chem. **42A**, 2762 (2003)
4. B. Dede, F. Karipcin, M. Cengiz, J. Hazard. Mater. **163**, 1148 (2009)
5. A.K. Mishra, N. Manav, N.K. Kaushik, Spectrochim. Acta A **61**, 3097 (2005)
6. M.G. Abd El Wahed, E.M. Nour, S. Teleb, S. Fahim, J. Therm. Anal. Calorim. **76**, 343 (2004)
7. M. Ak, D. Taban, H. Deligoz, J. Hazard. Mater. **154**, 51 (2008)
8. S. Karabocek, S. Güner, N. Karabocek, J. Inorg. Biochem. **66**, 57 (1997)
9. Y.M. Al-Hıari, B.A. Sweileh, Asian J. Chem. **18**, 2285 (2006)
10. N. Zanatta, S.H. Alues, H.S. Coelho et al., Bioorg. Med. Chem. **15**, 1947 (2007)
11. Z. Önal, İ. Yıldırım, Heterocycl. Commun. **13**, 113 (2000)
12. H.G. Aslan, Z. Onal, Med. Chem. Res. **23**, 2596–2607 (2014)
13. K.K. Anderson, in *Comprehensive Organic Chemistry*, vol. 3, ed. by D.N. Jones (Pergamon Press, Oxford, 1979), p. 345
14. S.L. Graham, T.H. Scholz, Synthesis **12**, 1031 (1986)
15. A. Boruah, M. Boruah, D. Prajapati, J.S. Sandhu, Synlett **1997**, 1253 (1997)
16. S. Iyer, A.K. Sattar, Synth. Commun. **28**, 1721 (1998)
17. W. Chan, Y.C. Berthelette, Tetrahedron Lett. **43**, 4537 (2002)
18. H.G. Aslan, S. Özcan, N. Karacan, Inorg. Chem. Commun. **14**, 1550 (2008)
19. H.G. Aslan, S. Özcan, N. Karacan, Spectrochim. Acta A Mol. Biomol. Spectrosc. **98**, 329 (2012)
20. A.G. Newcombe, Can. J. Chem. **33**, 1250–1255 (1955)
21. A.B.P. Lever, *Inorganic Electronic Spectroscopy*, 2nd edn. (Elsevier, Amsterdam, 1984)
22. S. Akkoç, Y. Gök, J. Iran. Chem. Soc. **11**, 1767–1774 (2014)
23. S. Akkoç, Y. Gök, İ.Ö. İlhan, V. Kayser, Beilstein J. Org. Chem. **12**, 81–88 (2016)